https://doi.org/10.5194/egusphere-2025-2849
Preprint. Discussion started: 4 July 2025

The Use of Newly Assimilated Photosynthates by Soil Autotrophic and Heterotrophic Respiration on a Diurnal Scale

Moeka Ono[1], Bhaskar Mitra[2], Benju Baniya[1], Dohee Kim[1], Asko Noormets[1]

[1]Department of Ecology and Conservation Biology, Texas A&M University, College Station, TX, United States
[2]Information and Computational Science Department, The James Hutton Institute, Aberdeen, UK

Correspondence to: Moeka Ono (mono@tamu.edu) and Asko Noormets (noormets@tamu.edu)

Abstract

The regulatory role of plant carbohydrate status and root exudation on soil CO_2 efflux has been demonstrated, yet the underlying mechanisms, particularly through root respiration, remain largely theoretical. In this study, we analyzed the cospectral variation of soil autotrophic (Ra) and heterotrophic (Rh) respiration components with key physiological and environmental factors, including gross primary productivity (GPP), photosynthetically active radiations (PAR), soil temperature (Ts) and volumetric water content (VWC), to evaluate their relative contributions in a subtropical mature shortleaf pine forest in the southern United States. The findings reveal a strong diurnal relationship between Rh and both GPP and PAR, in contrast to the weaker and more variable associations observed with Ra. This suggests that substrate availability was a key limitation of Rh on a diurnal basis, and that recently assimilated carbohydrates were directly discharged into the soil via root and mycorrhizal exudates. The consistent 2–4 hour time lag between Rh relative to GPP is consistent with the propagation rate of phloem pressure-concentration waves. While a diurnal peak in Rh-Ts covariance was also detected, the time lag of Rh in relation to Ts varied between positive and negative values, precluding this from being a causal relationship. Ra had a similarly strong cospectral peak with GPP as Rh, but with inconsistent lag, likely because of carbon availability from local starch reserves.

1 Introduction

In the global carbon (C) cycle, soil CO_2 efflux (SR) is a major terrestrial C flux, estimated at 89 Pg C $year^{-1}$ (range: 68–101 Pg C $year^{-1}$) (Hashimoto et al., 2023; Jian et al., 2021), approximately nine times greater than annual fossil fuel emissions (Friedlingstein et al., 2022), and serves as the primary pathway for returning plant-assimilated CO_2 to the atmosphere. SR arises from the combined respiration of plant roots, rhizosphere microbes, and mycorrhizal and free-living fungi, with carbohydrates (CHO) translocated from photosynthetic tissues playing an essential role in sustaining this flux (Kuzyakov & Gavrichkova, 2010). Autotrophic respiration (Ra), including root and mycorrhizal respiration, is, in principle, directly fueled by CHO translocated belowground (Fenn et al., 2010; Heinemeyer et al., 2012). Heterotrophic respiration (Rh), particularly rhizosphere microbes, is also linked to photosynthesis through above- and belowground detritus production and

https://doi.org/10.5194/egusphere-2025-2849
Preprint. Discussion started: 4 July 2025

rhizodeposition, including exudates that provide labile C inputs, which are estimated to be around 1–3% of a forest's net primary productivity (NPP) (Phillips et al., 2008; Yin et al., 2014). The recent demonstration of tight coupling between SR and GPP (Han et al., 2014; Heinemeyer et al., 2012; Mitra et al., 2019) suggests that the pattern is driven by root respiration as mediated by the diurnal fluctuation in plant CHO status. With Rh being further removed from the CHO source, the primary C inputs (i.e., detritus) varying on a seasonal scale, and reports of lower temperature sensitivity of Rh than Ra (Reichstein et al., 2005), it has often been viewed as a more invariable, baseline process. However, direct evidence for such differentiation remains limited. This challenges the conventional approach of modeling SR primarily as a function of soil temperature (Davidson et al., 2006) and moisture (Davidson et al., 1998; Li et al., 2008), as such models fail to account for diurnal variations in SR (Martin et al., 2012).

The allocation of CHO belowground depends on the relative strength of different C sinks in plants, which, in turn, may be restricted by water and nutrient availability (Jiang et al., 2020; Körner, 2015; Sevanto & Dickman, 2015), physiological state, and hormones (Herms & Mattson, 1992), all of which vary seasonally and respond to stresses (Gessler & Zweifel, 2024). As summarized in the "surplus carbon hypothesis" (Prescott et al., 2020), overwhelming evidence supports the view of a passive, sink-strength-driven nature of C allocation, with implications for C cycling and responses to stressors, such as drought and nutrient limitations (Prescott, 2022; Prescott et al., 2020). Surplus CHO, that are not used in aboveground growth and maintenance, can be stored locally (as starch or lipids), converted to secondary compounds, or translocated from leaves to belowground compartments, where they can support root and mycorrhizal growth, or be exuded into the soil. The sink-strength-driven allocation model implies that this process helps regulate CHO concentrations in cells, preventing them from reaching levels that could become toxic to cellular processes. However, quantifying the interactions between CHO translocation and CO_2 release remains challenging due to the complexity of these mechanisms.

The timescale and level of coupling between photosynthetic C uptake and soil processes are confounded by plant physiological processes that can introduce variable lags to C transport from leaves to different plant organs, including the sink strength of different tissues, mycorrhizal associations, and the rate of phloem transport (Canarini et al., 2019; Sevanto & Dickman, 2015), as well as by methodological effects. Much of our current understanding of C allocation originates from stable isotope labeling studies, in which the progressive detection of isotopically labeled C in different tissues has been tracked (e.g., Gessler et al., 2007; Högberg et al., 2008; Kodama et al., 2008; Wingate et al., 2010). These studies show that the newly assimilated C can be translocated from leaves of a tree to the roots on the order of a day or two (Mencuccini & Hölttä, 2010; Moyano et al., 2008). Yet, our earlier analysis (Mitra et al., 2019), as well as those of others (Vargas et al., 2011), detected a consistent cospectral peak between SR and CHO availability, indicated by photosynthetically active radiation (PAR) or net ecosystem exchange (NEE), on the order of hours, which is attributable to plant carbohydrate status responding via pressure-concentration waves (Thompson & Holbrook, 2004). Finally, additional and potentially variable lags may be introduced by soil heterotrophs, where the C subsidy by plant exudates may not only provide free substrate for their metabolism, but can also trigger priming

https://doi.org/10.5194/egusphere-2025-2849
Preprint. Discussion started: 4 July 2025

of the decomposition of old recalcitrant soil C, by providing energy (and possibly substrate) for the production of more resource-intensive enzymes (Jilling et al., 2021; Meier et al., 2017).

Here we report the coherence of Rh and Ra with key physiological and environmental drivers, gross primary productivity (GPP), PAR, soil temperature, and soil moisture, with the focus on the diurnal timescale. We hypothesized that GPP is the primary driver of diurnal variations in Ra, while soil temperature and moisture predominantly regulate Rh, with influences spanning diel and synoptic scales. Quantitative understanding of the coupling between respiration components and GPP may help address key remaining uncertainties in ecosystem carbon cycle models (Lawrence et al., 2019; O'Sullivan et al., 2022).

2 Materials and Methods

2.1 Study Site

The study was conducted at the US-CRK Ameriflux site, a fire-managed mature shortleaf pine forest in Davy Crockett National Forest, TX (31.4629 N, 95.3415 W), in a humid subtropical climate region. The average annual precipitation and annual temperature are 1148 mm and 19.1 ℃, respectively. The soil type at this site is classified as moderately well-drained Latex loam. The majority of fine root biomass (84%) was concentrated in the top 30 cm of soil at the site (Fig. S1). The site is maintained through biannual prescribed burning, and the recent burning took place in the winters of 2022 and 2024, although the fire's effect on the measurement area was minimal. The overstory vegetation within the study site is primarily dominated by shortleaf pine (*Pinus echinata*), with lesser amounts of loblolly pine (*Pinus taeda*), American sweetgum (*Liquidambar styraciflua*), and post oak (*Quercus stellata*). The stand average tree diameter at breast height was 33.1 ± 1.60 cm, the mean tree height was 25.8 ± 1.47 m, and the estimated aboveground biomass was 15.4 ± 0.06 kg m^{-2} $year^{-1}$ in 2021.

2.2 Continuous Soil Respiration Measurements

Continuous soil respiration measurements were conducted hourly from May 2022 through October 2024 using an infrared gas analyzer (LI-8100A, LI-COR Biosciences, Lincoln, NE, USA) equipped with three long-term chambers (LI-8100-101 and LI-8100-104, LI-COR Biosciences). Chambers were installed over shallow (5cm tall) or deep (30 cm) polyvinyl chloride (PVC) collars. Shallow collars were inserted 2–3 cm into the soil and used to quantify total soil CO_2 efflux (SR), while deep collars were inserted approximately 25 cm into the soil to sever roots and capture root-excluded heterotrophic soil CO_2 efflux (Rh). Collars were initially installed in April 2022 and relocated in April 2023, October 2023, and June 2024 to maintain effective root severance in deep collars (Ono et al., 2025). Only periods during which the CO_2 efflux ratio between paired deep and shallow collars had stabilized, validated against manual survey measurements across five surrounding study plots (Baniya et al., 2025), were included in the analysis. The paired shallow and deep collars were placed at similar microsites, at a similar distance (approx. 2–3 m) from the nearest tree, and ensuring that initial soil CO_2 efflux rates would not differ more than 10%. Aboveground vegetation within collars was clipped monthly to maintain bare-soil conditions. The spatial representativeness

https://doi.org/10.5194/egusphere-2025-2849
Preprint. Discussion started: 4 July 2025

of the single automated system was further supported by comparison with 25 pairs of similar paired collars at five study plots and measured for three years (Baniya et al., 2025). Autotrophic respiration (Ra) was estimated by the difference between SR and Rh during periods when Rh was deemed stable. The stable usable estimates of partitioned Rh (and Ra) occurred typically between 3 and 6 months after deep collar insertion. Soil CO_2 efflux declined during the first 2-3 months of the deep collar insertion as root internal carbohydrate reserves were being depleted. After about 6-8 months, the CO_2 efflux in the deep collars began to increase as the dead roots became additional substrate for heterotrophs (McElligott et al., 2016).

Six measurement periods (hereafter referred to as campaigns), each spanning approximately 3–4 weeks, were identified from the continuous dataset. They were determined by the simultaneous availability of high-quality GPP, Rs, Rh, PAR, Ts, and SWC data. The six campaigns included two early growing seasons (C1, C4), one late growing season (C5), and three dormant seasons (C2, C3, C6) (Table 1, Fig.1). The categorization into seasons was based on canopy leaf area index (LAI) and mean GPP values.

2.3 Micrometeorological Parameters

Photosynthetically active radiation (PAR) was measured half-hourly above the canopy at a height of 43 m (PQS1, Kipp & Zonen, Delft, Netherlands). Soil temperature (Ts) and volumetric water content (VWC) were recorded half-hourly at 5 cm depth with CS108 and CS650 probes, respectively (both by Campbell Scientific, Logan, UT, USA). Half-hourly gross primary productivity (GPP) was estimated by partitioning the net ecosystem exchange of CO_2 into GPP and ecosystem respiration using the nighttime partitioning approach in the "Reddyproc" package in R (Wutzler et al., 2022). Specific details of eddy covariance data processing are reported by Baniya et al. (2025). All parameters were aggregated to hourly values for analysis.

The leaf area index (LAI) at the site was extracted from the Moderate Resolution Imaging Spectroradiometer (MODIS; MCD15A3H Version 6.1), which provides 4-day composite estimates for a 500-meter pixel centered on the study site (Myneni et al., 2021). Peak LAI estimates were verified against on-site measurements with a LAI-2000 Plant Canopy Analyzer (LI-COR Biosciences) in August 2023. Both estimates matched within 0.2 m^2 m^{-2} (data not shown).

2.4 Data Analysis

All data analyses were performed in R (version 4.3.3) (R Core Team, 2024) and implemented in RStudio (version 2023.12.1) (Posit team, 2024).

2.4.1 Quality Control of Soil Respiration Components

Occasional abnormal spikes in the soil respiration data time series were observed, often due to gas analyzer failure or interference from small animals. To ensure the data quality for subsequent analyses, these anomalies were removed using the

https://doi.org/10.5194/egusphere-2025-2849
Preprint. Discussion started: 4 July 2025

following quality control criteria: (1) poor model fit for flux calculation ($R^2 < 0.975$), (2) high coefficient of variation (CV > 1.9), (3) negative flux values, and (4) insufficient flow rate.

2.4.2 Spectral Analysis

We analyzed the wavelet spectra of soil respiration components (Ra and Rh, or their residuals, r_{Ra} and r_{Rh}; Section 2.4.3) and their cospectrum with environmental and physiological drivers (GPP, PAR, Ts, and VWC) in the time-frequency domain. Continuous wavelet transformation was performed using the Morlet wavelet as the basis function (Grinsted et al., 2004). We applied wavelet transformation (WT) and cross-wavelet transformation (XWT) analyses, following the methodological framework described by Mitra et al. (2019).

For cospectral analysis, time series data were normalized to zero mean and unit variance, and occasional gaps were filled using zero padding. To align with the temporal scales of interest, the analysis focused on frequencies corresponding to time intervals from 6 hours to 64 days. For the phase angle analysis between effects (i.e., Rh and Ra) and drivers, we focused on the diurnal frequency range (0.5 to 1.5 days). Phase differences within this range were averaged but included only when the spectral peak at the 1-day period was statistically significant ($p < 0.1$). Daily mean phase angles were then converted to time lags (in hours) using Lag (hours) = (mean phase angle × 24) / (2π). To prevent introducing artifacts, phase angle values during padded gaps were excluded. The statistical significance of WT and XWT analyses was evaluated within the cone of influence (COI) at a 5% significance level. The cospectral analysis was performed using the "analyze.coherency" function in the "WaveletComp" package in R (Roesch & Schmidbauer, 2018).

2.4.3 Residual Analysis

We also analyzed the temperature- and GPP- (or PAR-) controlled components of Ra and Rh by first removing the temperature dependence by exploring the cospectra of the potential drivers with the residuals of the measured and modeled Ra and Rh (r_{Ra} and r_{Rh}) (Liu et al., 2006; Vargas et al., 2011). Ra and Rh were modeled using the Q_{10} function (van't Hoff (1898) as cited in Lloyd and Taylor (1994)):

$$R_{model} = R_{20} \times Q_{10}^{\frac{T_S - 20}{10}}, \quad (1)$$

where R_{model} is the modeled respiration component at soil temperature (T_s) at 5 cm depth, R_{20} is the reference respiration at 20 °C, and Q_{10} is the temperature sensitivity coefficient. Given that spectral analysis of Ts revealed diurnal and weekly peaks across campaigns (Figs. 3M-R; see section 3.2), coefficients (R_{20} and Q_{10}) were derived separately for each day and a weekly rolling window. The corresponding residuals were denoted as r_{Rh_day} (or r_{Ra_day}) and r_{Rh_week} (or r_{Ra_week}), respectively. Coefficients were estimated by minimizing the residual sum of squares through nonlinear least-squares analysis using the "nls_table" function in the "forestmangr" package in R (Braga et al., 2023).

https://doi.org/10.5194/egusphere-2025-2849
Preprint. Discussion started: 4 July 2025

3 Results

3.1 Soil Respiration and Environmental Conditions

Across the six measurement campaigns, SR ranged from 1.69 ± 0.81 to 5.05 ± 1.03 µmol CO_2 m^{-2} s^{-1}, Rh from 1.05 ± 0.40 to 2.46 ± 0.32 µmol CO_2 m^{-2} s^{-1} and Ra 0.43 ± 0.38 to 2.70 ± 0.84 µmol CO_2 m^{-2} s^{-1} (Table 1, Figs. 1A-D). Maximum effluxes for SR and Ra were recorded in C1, which corresponded to the highest GPP and LAI (Table 1). On the other hand, lower SR, Rh, and Ra were observed during dormant-season campaigns (C2, C3, and C6). Rh consistently accounted for the majority of SR, contributing 59-86% across campaigns, except for C1, when its contribution was 47%. Notably, VWC during C3 and C4 was among the highest, driven by sustained rainfall in early 2024.

https://doi.org/10.5194/egusphere-2025-2849
Preprint. Discussion started: 4 July 2025

Table 1. Mean site conditions and fluxes during the six measurement campaigns (Mean ± standard deviation). Soil temperature (Ts; °C) and volumetric water content (VWC; %) at a depth of 5 cm, total soil respiration (SR; µmol m^{-2} s^{-1}), heterotrophic respiration (Rh; µmol m^{-2} s^{-1}), autotrophic respiration (Ra; µmol m^{-2} s^{-1}), the ratio of Rh to SR (Rh:SR; unitless), daylight-period gross primary productivity (GPP; µmol CO_2 m^{-2} s^{-1}), and leaf area index derived from MODIS (LAI; m^2 m^{-2}). Campaigns conducted during active growing seasons are marked with an asterisk (*).

Campaign	Date	Ts	VWC	SR	Rh	Ra	Rh:SR	GPP	LAI
1*	2022-05-22 ~ 2022-06-09	24.1 ± 2.31	24.2 ± 1.78	5.05 ± 1.04	2.35 ± 0.45	2.70 ± 0.84	0.47 ± 0.08	14.3 ± 2.94	4.18 ± 0.79
2	2023-03-15 ~ 2023-04-05	16.4 ± 2.57	23.4 ± 2.95	1.69 ± 0.81	1.05 ± 0.40	0.51 ± 0.43	0.71 ± 0.15	9.05 ± 2.53	1.68 ± 0.15
3	2024-03-03 ~ 2024-03-31	16.6 ± 2.05	42.6 ± 0.66	1.79 ± 0.63	1.38 ± 0.39	0.44 ± 0.38	0.79 ± 0.16	8.31 ± 2.01	1.17 ± 0.40
4*	2024-04-01 ~ 2024-04-27	19.2 ± 1.93	43.0 ± 0.52	2.15 ± 0.68	1.88 ± 0.42	0.43 ± 0.40	0.84 ± 0.18	11.6 ± 2.29	1.77 ± 0.90
5*	2024-09-03 ~ 2024-09-30	24.7 ± 2.17	10.4 ± 2.14	4.20 ± 0.54	2.47 ± 0.32	1.73 ± 0.42	0.59 ± 0.07	11.1 ± 1.76	2.11 ± 0.41
6	2024-10-01 ~ 2024-10-31	21.8 ± 2.62	4.11 ± 0.90	2.10 ± 0.50	1.78 ± 0.32	0.32 ± 0.31	0.86 ± 0.11	8.21 ± 1.85	1.75 ± 0.29

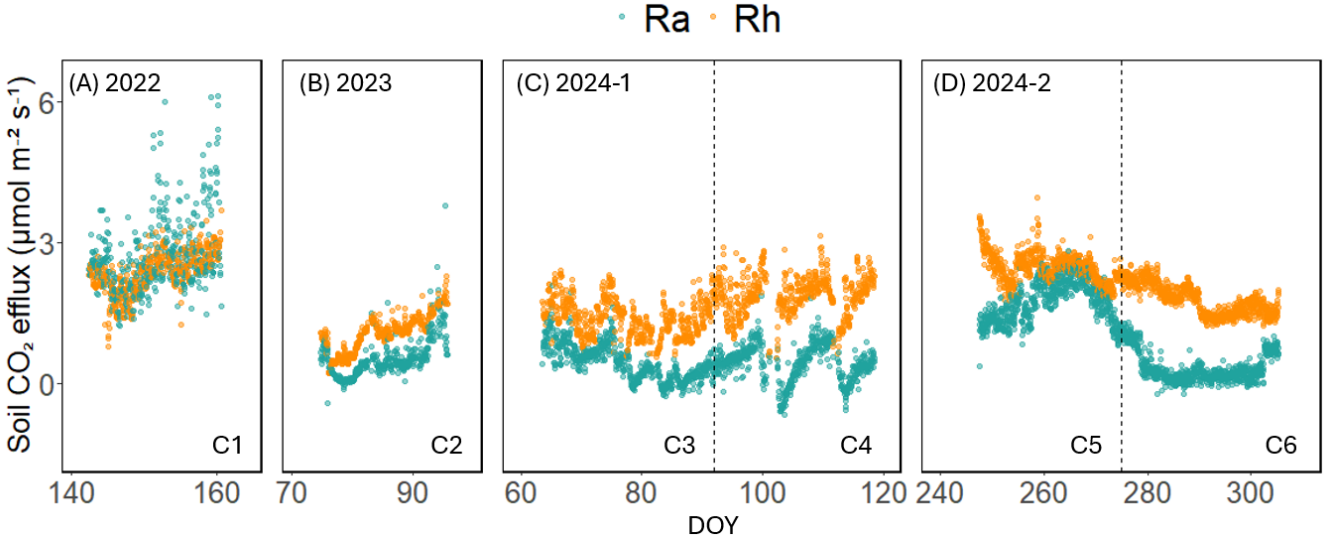

Figure 1. Hourly time series of soil autotrophic respiration (Ra, green) and heterotrophic respiration (Rh, orange) in µmol m^{-2} s^{-1} across six measurement campaigns (C1-C6) at the US-CRK between 2022 and 2024 (A-D).

https://doi.org/10.5194/egusphere-2025-2849
Preprint. Discussion started: 4 July 2025

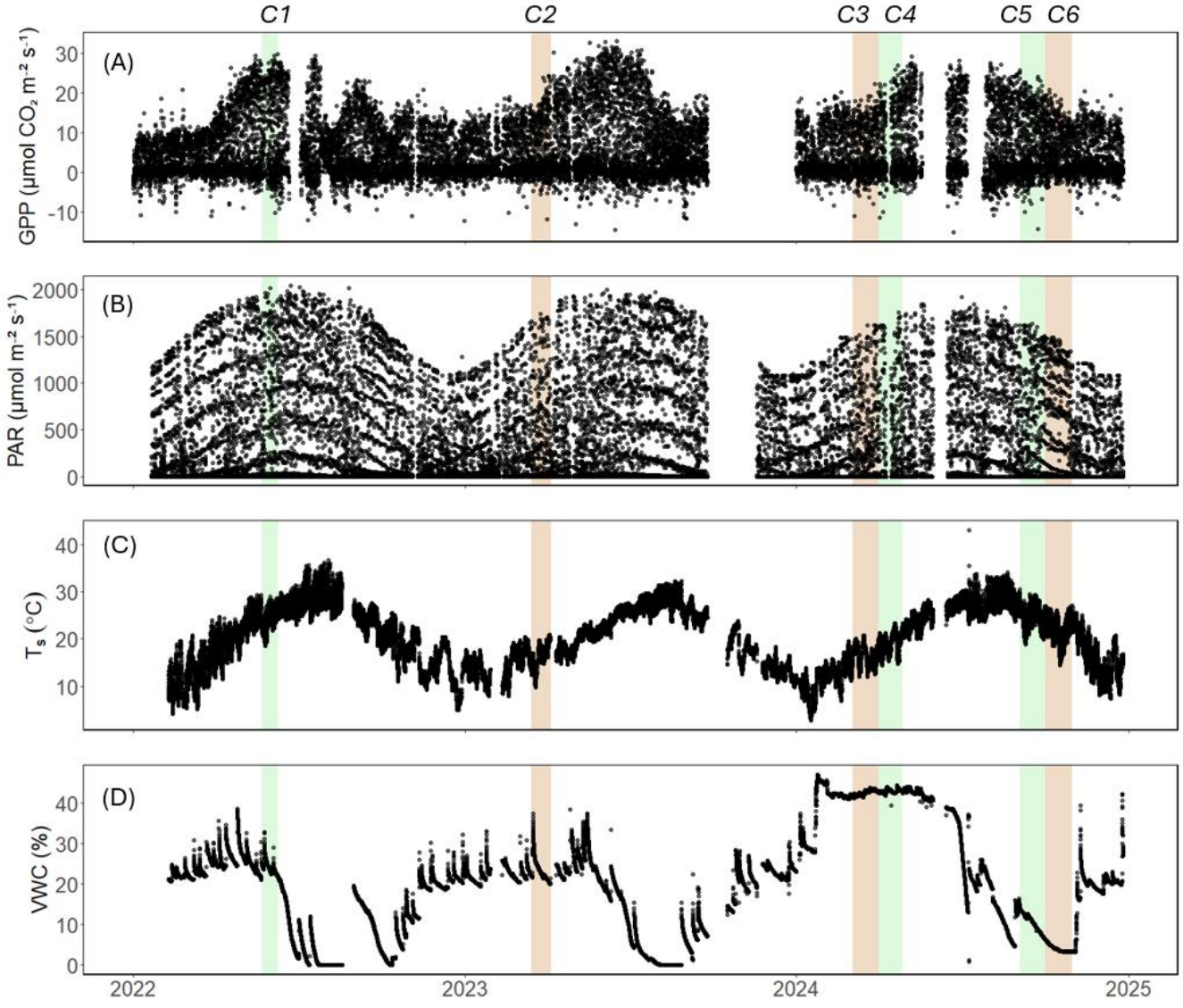

Figure 2. Hourly time series of (A) gross primary productivity (GPP; µmol CO_2 m^{-2} s^{-1}), (B) photosynthetically active radiation (PAR; µmol m^{-2} s^{-1}), (C) soil temperature (Ts; °C), and (D) volumetric water content (VWC; %) at the US-CRK site from 2022 to 2024. Shaded regions denote the six soil respiration measurement campaigns (C1-C6); green indicates active growing season campaigns, while brown indicates dormant season campaigns.

https://doi.org/10.5194/egusphere-2025-2849
Preprint. Discussion started: 4 July 2025

3.2 Spectral and Cospectral Characteristics

GPP and PAR consistently exhibited significant subdiurnal and strong diurnal spectral peaks across all six campaigns (Figs. 3A–L). In contrast, Ts displayed both significant diurnal and synoptic peaks, with the latter ranging from weekly to monthly timescales, while VWC varied mostly at synoptic scale (Figs. 3M–X). Rh showed significant diurnal spectral peaks in all campaigns, with more pronounced and distinct peaks during the growing season (C1, C4, and C5) and C3 (Figs. 4A–F). Synoptic peaks in Rh were also detected. Spectral analysis of Ra showed strong, significant diurnal peaks in C1 and weak but still significant diurnal peaks in C2, C3, and C5, along with detectable synoptic peaks (Figs. 5A–F).

Cospectral analysis showed that Rh exhibited significant diurnal peaks with GPP and PAR across all campaigns, with stronger diurnal peaks during the growing seasons (C1, C4, and C5) and in C3 (Figs. 4G–R, 6A–L). Ra also exhibited significant diurnal peaks with GPP and both subdiurnal and diurnal peaks with PAR, particularly during C1 and C5 (Figs. 5G–R, 7A–L). Although Ra exhibited relatively stronger cospectral diurnal strength in C1 and C2, the diurnal cospectral strength of Rh with GPP and PAR exceeded that of Ra by a factor of 1.2–2.6 times in C3–C6.

Cospectral analysis with Ts demonstrated both significant diurnal and synoptic peaks for both Rh and Ra across campaigns (Figs. 4S–X, 5S–X). Notably, in C2, C3, and C4, cospectral peaks at weekly timescales were stronger than those at the diurnal timescale. While peaks extending beyond monthly timescales were observed for both Rh and Ra with Ts, they fell outside the cone of significance and were excluded from further interpretation. Rh and Ra also exhibited cospectral peaks with VWC at synoptic scales (weekly to monthly). Significant diurnal peaks were detected only during C1, C3, and C4, but these were generally weaker and less consistent than those observed with GPP, PAR, and Ts (Figs. 4Y–A4, 5Y–A4). Overall, their cospectral peaks at weekly scales were stronger than diurnal-scale peaks.

Cospectral analysis of model residuals (r_{Rh_day} and r_{Ra_day}, as well as r_{Rh_week} and r_{Ra_week}) with GPP and PAR showed overall patterns consistent with those of Rh and Ra. Diurnal peaks of r_{Rh_day} and r_{Rh_week} with GPP and PAR were consistently pronounced and significant across campaigns (Figs. S2 G–R, S6 G–R). Both r_{Ra_day} and r_{Ra_week} also exhibited consistently significant diurnal peaks with GPP and PAR (Figs. S3 G–R, S7 G–R), with particularly strong peaks of r_{Ra_day} observed during C5 and C6 (Figs. S3 K, L).

https://doi.org/10.5194/egusphere-2025-2849
Preprint. Discussion started: 4 July 2025

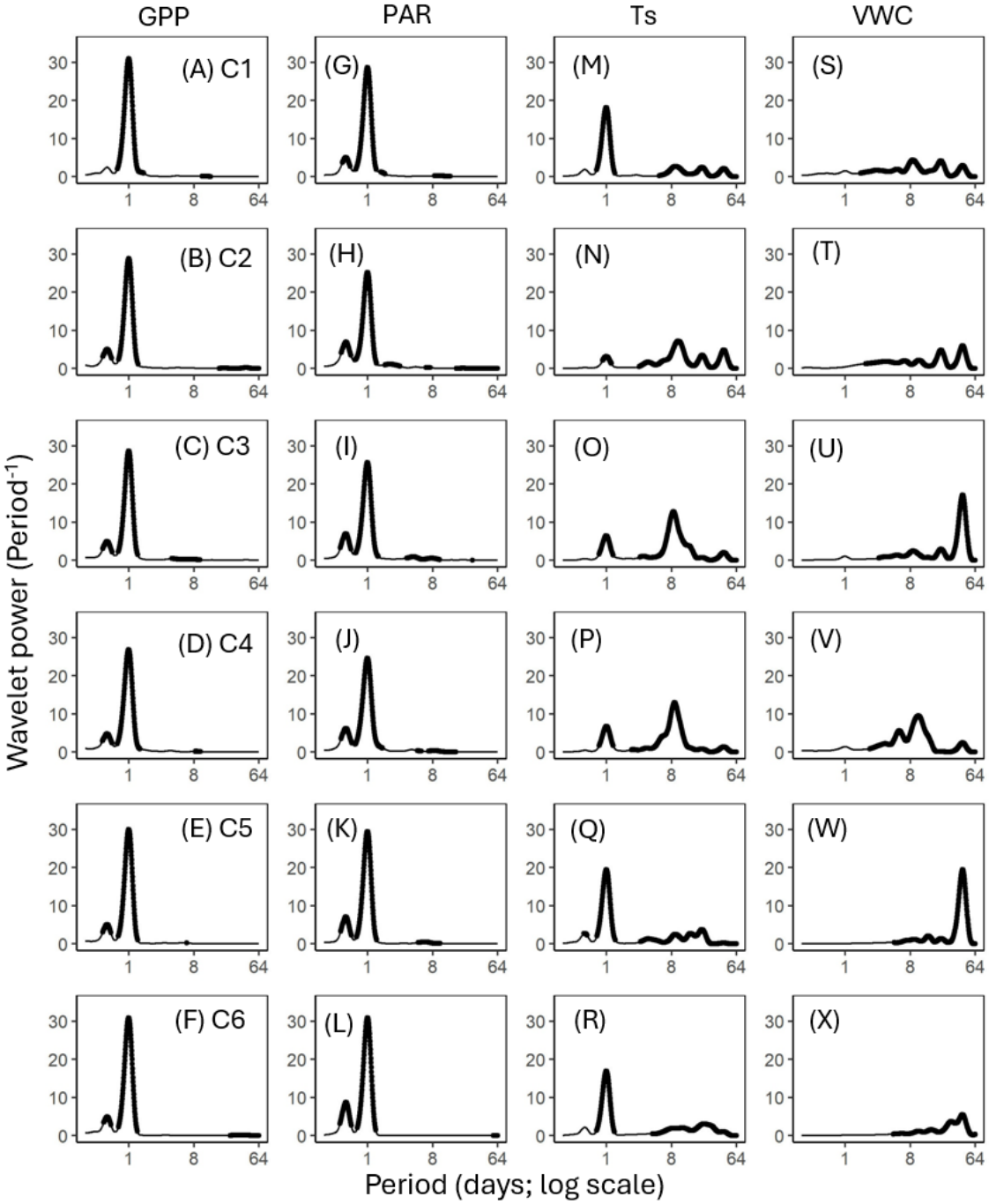

Figure 3. Average wavelet power in the frequency domain generated from the wavelet transformation of gross primary productivity (GPP; A–F), photosynthetically active radiation (PAR; G–L), soil temperature (Ts; M–R), and volumetric water content (VWC; S–X) at 5-cm depth for six campaigns (C1–C6) at US-CRK. The bold contours indicate areas with significant coherence at the 5% level against white noise.

https://doi.org/10.5194/egusphere-2025-2849
Preprint. Discussion started: 4 July 2025

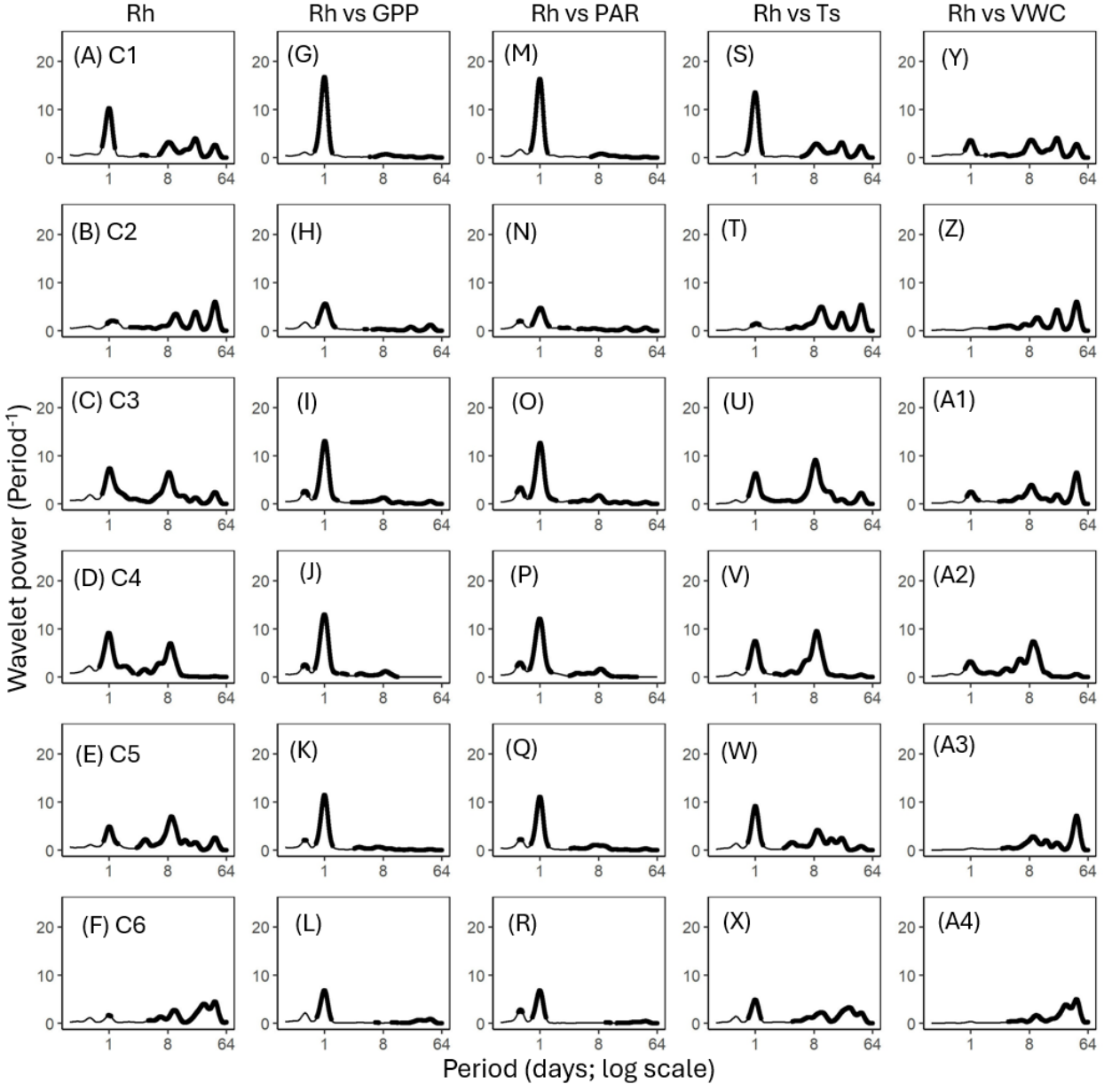

Figure 4. Average wavelet power in the frequency domain generated from the wavelet transformation of heterotrophic respiration (Rh; A–F) for six campaigns (C1–C6) at US-CRK. Average wavelet power in the frequency domain generated from the cross-wavelet transformation of heterotrophic respiration (Rh) against gross primary productivity (GPP; G–L), photosynthetically active radiation (PAR; M–R), soil temperature (Ts; S–X), and volumetric water content (VWC; Y–A4) at 5-cm depth for six campaigns at the US-CRK site. The bold contours indicate areas with significant coherence at the 5% level against white noise.

https://doi.org/10.5194/egusphere-2025-2849
Preprint. Discussion started: 4 July 2025

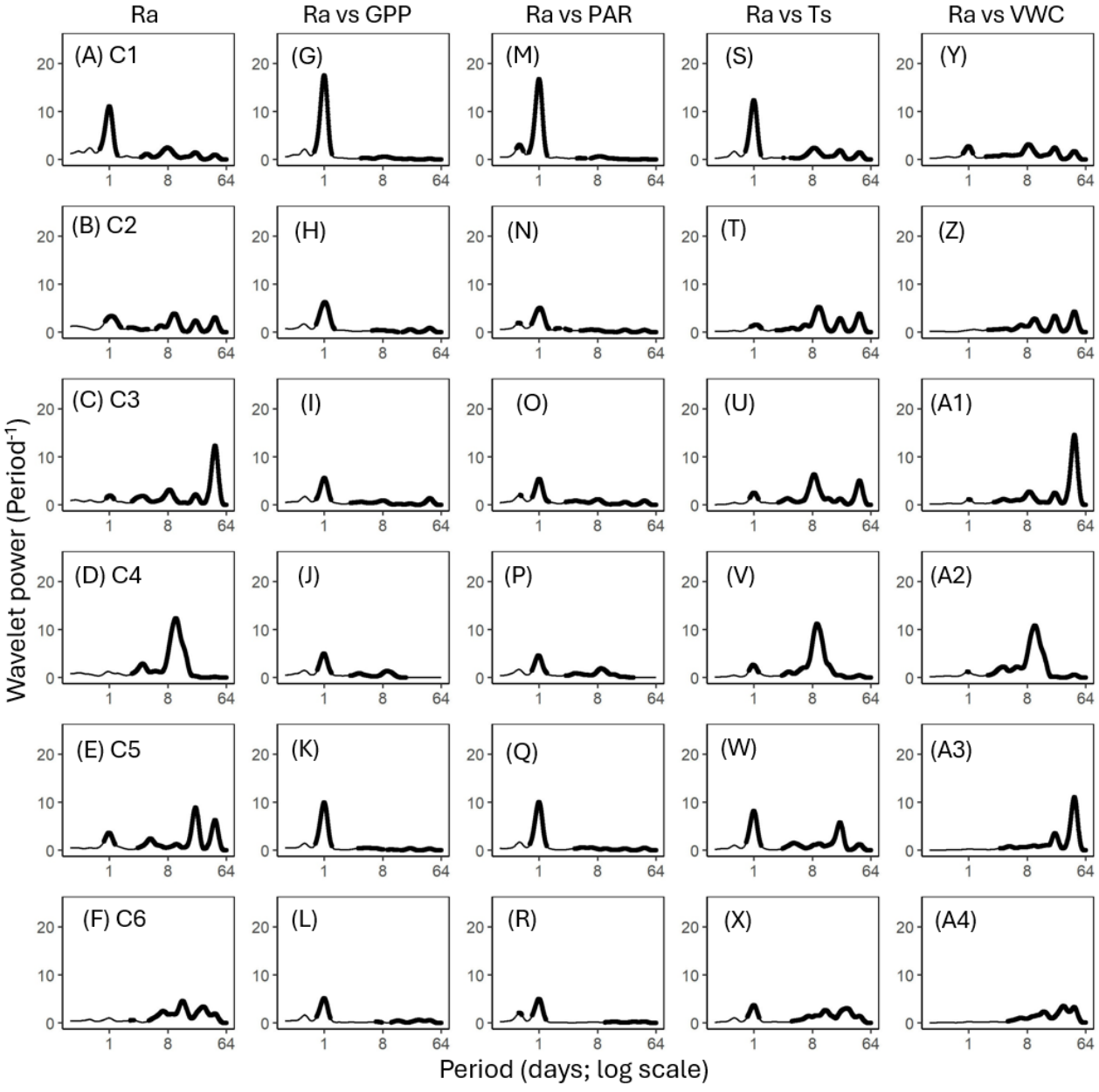

Figure 5. Average wavelet power in the frequency domain generated from the wavelet transformation of autotrophic respiration (Ra; A–F) for six campaigns (C1–C6) at US-CRK. Average wavelet power in the frequency domain generated from the cross-wavelet transformation of heterotrophic respiration (Rh) against gross primary productivity (GPP; G–L), photosynthetically active radiation (PAR; M–R), soil temperature (Ts; S–X), and volumetric water content (VWC; Y–A4) at 5-cm depth for six campaigns at the US-CRK site. The bold contours indicate areas with significant coherence at the 5% level against white noise.

https://doi.org/10.5194/egusphere-2025-2849
Preprint. Discussion started: 4 July 2025

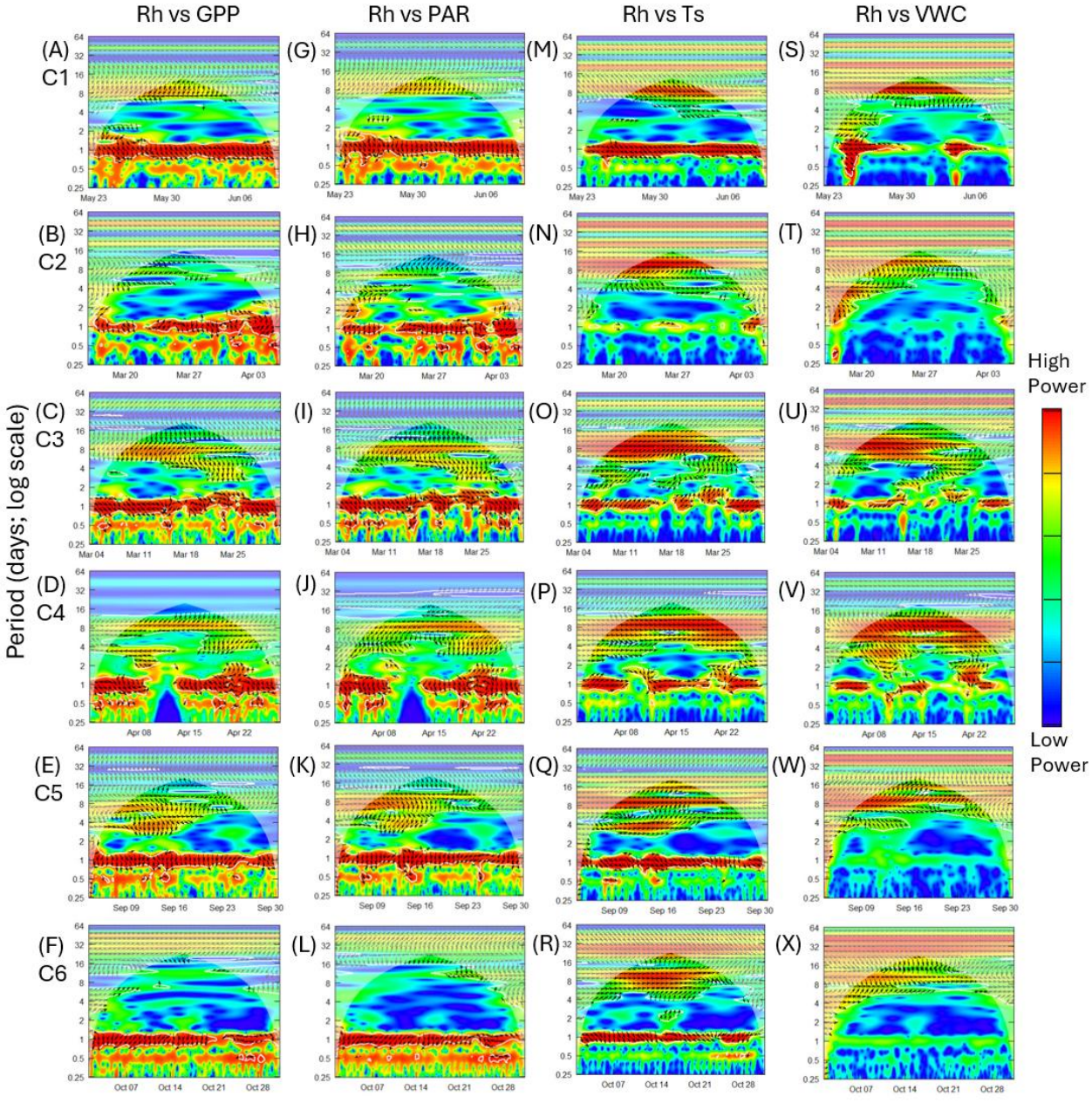

Figure 6. Heatmaps of the cross-wavelet transformation (XWT) of heterotrophic respiration (Rh) against gross primary productivity (GPP; A–F), photosynthetically active radiation (PAR; G–L), soil temperature (Ts; M–R), and volumetric water content (VWC; S–X) for six measurement campaigns (C1–C6) at US-CRK. Arrows pointing to the right and left represent positive and negative correlations, respectively, without lag. Arrows pointing up-left (positive correlation) and down-right (negative correlation) indicate the response component lags behind the driver, while arrows pointing up-right and down-left indicate that the driver lags behind the response component. The 5% significance level of the XWT analysis was generated within the cone of influence (COI) against white noise and identified by white contour lines. COI within the heat plot is identified with a light shade.

https://doi.org/10.5194/egusphere-2025-2849
Preprint. Discussion started: 4 July 2025

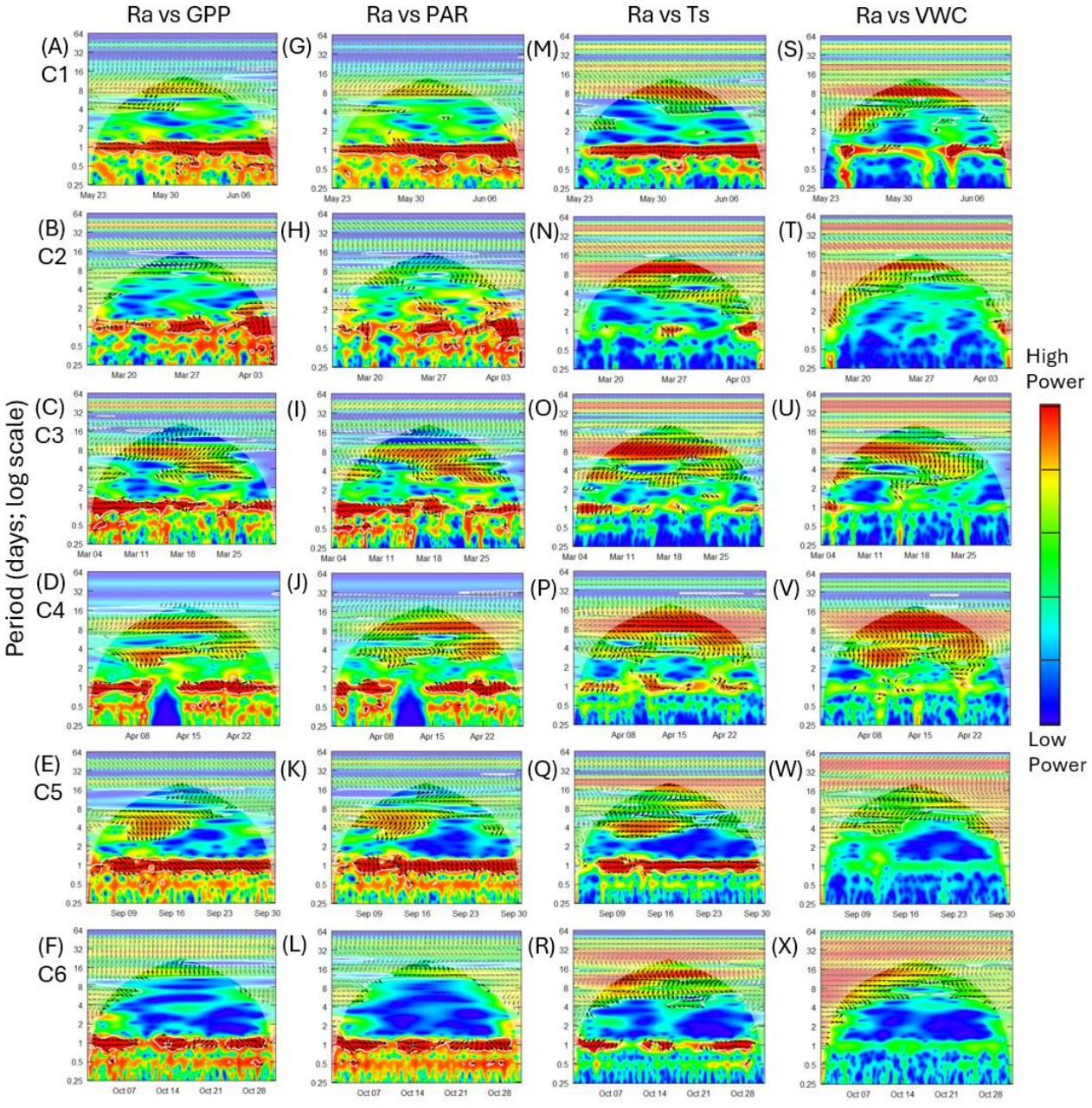

225 **Figure 7. Heatmaps of the cross-wavelet transformation (XWT) of autotrophic respiration (Ra) against gross primary productivity (GPP; A–F), photosynthetically active radiation (PAR; G–L), soil temperature (Ts; M–R), and volumetric water content (VWC; S–X) for six measurement campaigns (C1–C6) at US-CRK. Arrows pointing to the right and left represent positive and negative correlations, respectively, without lag. Arrows pointing up-left (positive correlation) and down-right (negative correlation) indicate the response component lags behind the driver, while arrows pointing up-right and down-left indicate that the driver lags behind**
230 **the response component. The 5% significance level of the XWT analysis was generated within the cone of influence (COI) against white noise and identified by white contour lines. COI within the heat plot is identified with a light shade.**

https://doi.org/10.5194/egusphere-2025-2849
Preprint. Discussion started: 4 July 2025

3.3 Phase Analysis

At the diurnal frequency range, the phase differences between Rh and both GPP and PAR revealed consistent lag patterns, with Rh lagging behind GPP by 1.7–4.2 hours and behind PAR by 2.4–4.3 hours across campaigns (Fig. 8A, B). In contrast, the phase relationships between Ra and GPP or PAR were more variable, with lag-lead times ranging from -1.8 to +4.8 hours for GPP and -3.3 to +5.7 hours for PAR, showing inconsistent patterns (Fig. 8D, E). Phase angle analysis using model residuals showed similar results, where r_{Rh_day} lagged GPP by -3.5 ± 0.42 hours on average, except during C2, which exhibited a slight lead of +0.64 ± 2.8 hours, and r_{Rh_week} lagged GPP by -5.7 to -0.02 hours (Figs. S10A, S11A). In contrast, r_{Ra_day} and r_{Ra_week} exhibited greater variability, with lag-lead times ranging from -1.9 to 2.1 hours and from +0.20 to 3.9 hours, respectively (Figs. S10D, S11D). The phase angles between Ts and Rh or Ra also varied, ranging from -3.8 to +2.2 hours for Rh and -3.9 to +1.5 hours for Ra, indicating an inconsistent lag-lead relationship at the diurnal timescale (Figs. 8C, F). Ts consistently lagged behind GPP and PAR by 3.5 ± 1.1 hours and 4.6 ± 1.3 hours, respectively, across all campaigns (Fig. S11).

https://doi.org/10.5194/egusphere-2025-2849
Preprint. Discussion started: 4 July 2025

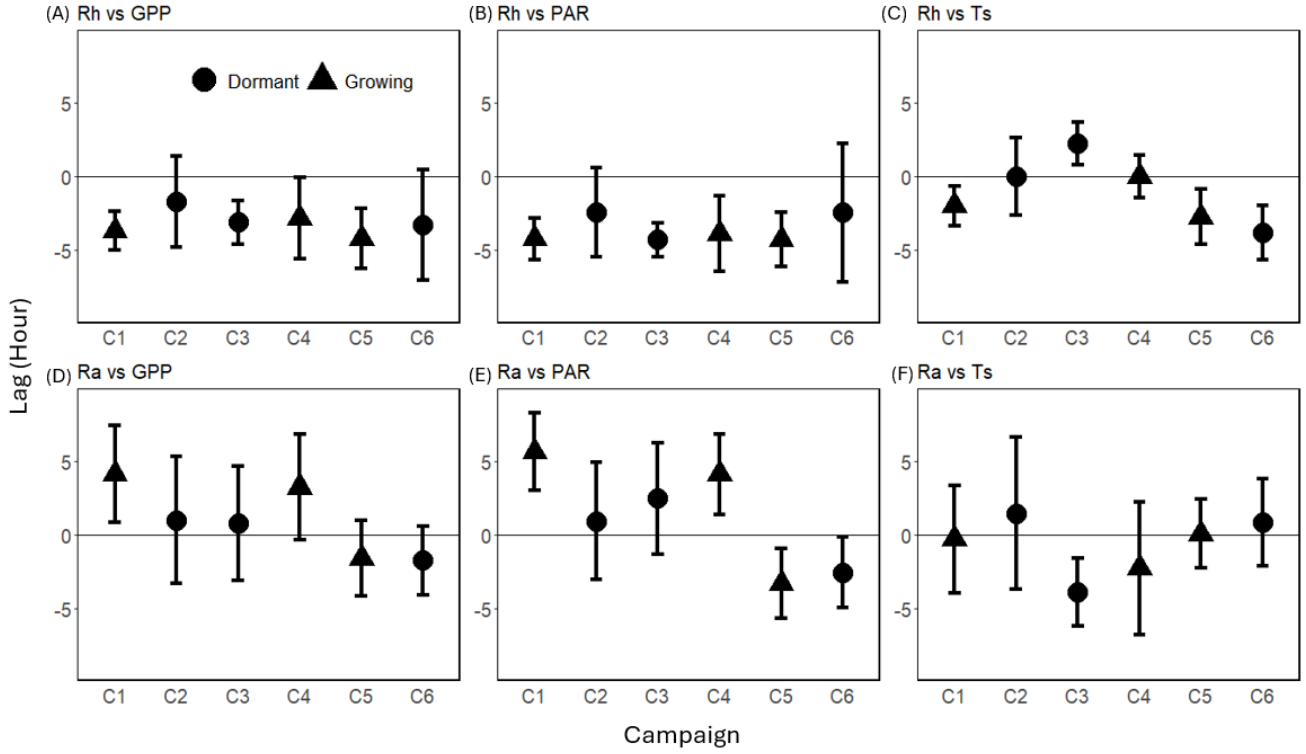

Figure 8. Mean time lag (± standard deviation) between heterotrophic respiration (Rh) in relation to (A) gross primary productivity (GPP), (B) photosynthetically active radiation (PAR), and (C) soil temperature (Ts), and between autotrophic respiration (Ra) with (D) GPP, (E) PAR, and (F) Ts at the diurnal frequency range (0.5 to 1.5 days) across six measurement campaigns (C1–C6). Phase differences were averaged over the diurnal frequency range and included only when the 1-day spectral peak was significant ($p < 0.1$). Round dots represent dormant season campaigns, while triangles represent growing season campaigns. Positive lag values indicate that respiration preceded the corresponding driver, while negative values indicate that respiration lagged behind the driver.

https://doi.org/10.5194/egusphere-2025-2849
Preprint. Discussion started: 4 July 2025

4 Discussion

4.1 Limitations and Uncertainties

This study lacks true replication, as measurements were conducted at a single system location. However, we report data from six measurement campaigns that span different seasons, vegetation physiological states, and soil water availabilities. The spatial representativeness of the continuous autochamber measurements of soil respiration measurements was validated against monthly manual survey measurements from 25 pairs of control and root exclusion collars located in five study plots over three years. A representativeness analysis (Baniya et al., 2025) indicated that the temporal dynamics of the SR, Ra, and Rh, as well as the heterotrophic fraction, were similar among all measurement locations, but the absolute magnitude of SR was slightly greater in plots with greater understory cover.

The partitioning of SR to Ra and Rh using the root exclusion method has its own limitations (Bond-Lamberty et al., 2011), and the partitioned fluxes are not independent. Measuring Rh separately from Ra (root severing approach) may give somewhat distorted Ra:Rh ratios. In the real world, these components interact with one another, and CHO-driven priming is omnipresent. In the current study, Rh should have been separated from root activity and diurnal fluctuations in CHO supply, but somehow (either by root and mycorrhizal hyphae ingrowth from below or root activity below the collar), the temporal dynamics of root-excluded soil were coupled more tightly than the estimated Ra.

4.2 Multitemporal Relationship of Rh and Ra with GPP, PAR, Ts, and VWC

The initial hypothesis that Ra would be more sensitive than Rh to GPP on a diurnal scale was not supported by the results. Instead, Rh and r_{Rh} demonstrated strong diurnal correlations with both GPP and PAR, as evidenced by distinct diurnal cospectral peaks (Figs. 4G–R, S2 G–R, S6 G–R) and heatmaps (Figs. 6A–L, S4 A–L, S8 A–L). The overall stronger diurnal cospectral relationship between Rh and GPP, compared to that of Ra and GPP, along with the consistent lag of Rh relative to GPP, rather than the more variable lag-lead patterns observed in Ra-GPP, suggests that the diurnal cycle of plant carbohydrate status was a key limiting factor for Rh, but was less pronounced for Ra. While Ra and r_{Ra} also exhibited a diurnal pattern with GPP, particularly during C5 and C6 (Figs. 5K–L, S3 K–L), the consistency was not observed across campaigns, suggesting that tissue carbon status may have been buffered by starch hydrolysis to meet the local energy and material demands (Zweifel et al., 2021). The strong response of Rh to plant C status during all measurement campaigns indicates an opportunistic microbial community. This contrasts with the interpretation of some earlier studies of total soil CO_2 efflux (SR) at different distances from trees, where the higher fluxes adjacent to trees were attributed to Ra (Savage et al., 2013; Tang et al., 2005) (further discussed in Section 4.3), as well as our own earlier spectral analysis (Mitra et al., 2019).

The observed 2–4 hour lag of Rh relative to GPP at the diurnal scale is consistent with previously reported rates of pressure-concentration wave propagation in the phloem (Kuzyakov & Gavrichkova, 2010; Mencuccini & Hölttä, 2010). Therefore, we

https://doi.org/10.5194/egusphere-2025-2849
Preprint. Discussion started: 4 July 2025

interpret it as a change in C availability (C status) in roots, with a likely pulse of exudation that triggered an increase in Rh within hours of enhanced photosynthetic activity, even though the mass flow of assimilates may occur over longer timescales.

Phase angle differences between Ra and Rh with Ts showed mixed lag and lead relationships. Notably, in C1 and C5, the lag of Rh relative to Ts (2.0 and 2.7 hours, respectively; Fig. 8C) was shorter than its lag relative to GPP (3.6 and 4.2 hours, respectively; Fig. 8A), suggesting a functional connection between them (Mitra et al., 2019). However, the greater cospectral peak height of Rh with GPP than with Ts (16.7 vs 13.5 period^{-1} in C1, and 11.4 vs 9.1 period^{-1} in C5; Figs. 4G, S, K, W) suggests that carbohydrate transfer had a greater influence on Rh diurnal dynamics.

4.3 Implications and Future Considerations

The consistently strong cospectral peaks between Rh and GPP suggest that surplus photosynthates, not immediately allocated to plant growth, are exuded into the soil, where they appear to support the activity of the opportunistic microbial community. Ecosystem scale estimates of the magnitude of root exudation remain difficult to quantify, but at the current study site, the overall allocation to non-structural carbon compounds exceeded 100 g C month^{-1} in some months (Baniya et al., 2025). How much of it was retained in plants as storage compounds and how much was exuded into the soil, and whether these can be derived from the diurnal magnitudes of each flux (Fig. 1), remains to be determined, but there appears to be ample C available to support the exudation.

These results contrast with earlier studies (e.g., Heinemeyer et al., 2012; Savage et al., 2013; Tang et al., 2005) that reported stronger correlations between root- or mycorrhizal-derived respiration and photosynthetic activity (e.g., GPP, NEE) compared to respiration derived from soil organic matter. However, these studies were conducted in temperate and Mediterranean deciduous forests, which may differ in carbon allocation strategies from the subtropical conifers that predominate our current study site. Additionally, Savage et al. (2013) and Tang et al. (2005) compared under-tree and open-area respiration to assess the contributions of soil respiration components. In contrast, our current study site was a complex forest with consistent tree cover and vigorous understory, with root exclusion collars placed 2–3 m from the nearest trees, where heterotrophic respiration likely included both rhizosphere priming and soil organic matter decomposition. Given that heterotrophic respiration does not occur in isolation from autotrophic processes but can respond dynamically to the diurnal supply of CHO, this methodological difference may explain the strong correlation observed between Rh and GPP in our study.

Our findings also align with the “surplus C theory” (Prescott, 2022; Prescott et al., 2020). During periods of high photosynthetic activity early in the growing season, or during dormant periods when the demand for photosynthates for plant growth and reproduction is limited, surplus carbohydrates may be discharged into the soil, potentially priming the turnover of soil organic carbon (Kuzyakov, 2010). At our mature pine forest site, the measurement periods, except for C1, corresponded to lower plant biomass production and positive non-structural carbon accumulation (Baniya et al., 2025). It is therefore plausible that surplus

https://doi.org/10.5194/egusphere-2025-2849
Preprint. Discussion started: 4 July 2025

C not allocated to growth or metabolism during these times could be exuded. Similar mechanisms have been reported in studies of mycelial respiration in boreal pine forest stands (Hagenbo et al., 2019) and under elevated CO_2 conditions in mature forest ecosystems (Jiang et al., 2020; Klein et al., 2016). The magnitude of exudation flux at different physiological states (as captured by the campaigns in the current study) remains to be determined. The changing magnitudes and diurnal amplitudes of both Ra and Rh (Fig. 1) could be caused by both environmental and physiological constraints, and carbon allocation to different plant compartments likely responds to both. Future research will incorporate diel measurements of carbohydrate concentrations in tree and root tissues, isotopic partitioning of soil respiration, and multi-season campaigns to further evaluate the mechanisms underlying these observations.

5 Conclusion

In conclusion, cospectral analyses using wavelet transformations showed that Rh and Ra respond to GPP, PAR, soil temperature, and soil moisture at different temporal scales. The diurnal variation of SR was primarily attributed to the dynamics of Rh, which, in turn, exhibited a consistent cospectral relationship with GPP. Ra also exhibited covaried with GPP, as well as soil temperature, but exhibited more variable and inconsistent time lags. These findings highlight the tight coupling between plant carbon status and soil microbial activity on a diurnal scale.

https://doi.org/10.5194/egusphere-2025-2849
Preprint. Discussion started: 4 July 2025

Code and data availability. Meteorological data at the US-CRK can be downloaded from the Ameriflux database (Noormets, 2024). Continuous soil respiration data and all the code files for the analyses in this manuscript can be found on GitHub via https://github.com/moekaono/CRK_cont_SR.

Author contribution. MO: Writing – original draft, Visualization, Methodology, Investigation, Software, Formal analysis, Data curation, Conceptualization. BM: Writing – review & editing, Supervision, Methodology, Investigation, Software, Validation, Conceptualization. BB: Software, Investigation, Data curation, Writing – review & editing. DK: Data curation, Writing – review & editing. AN: Writing – review & editing, Supervision, Resources, Validation, Project administration, Methodology, Investigation, Funding acquisition, Conceptualization.

Competing interests. The authors declare that they have no conflict of interest.

Acknowledgments. Blaize Britton, Clement Sarpong, Malik Nkrumah, and Seth Massery assisted with soil sampling and soil CO_2 efflux measurements. MO was supported by the ITO Foundation and the McMillan-Ward Fellowship. DK and BB were supported by the Native Plant Society of Texas.

Financial support. This project was supported by USDA NIFA (award #: 2023-67019-40537), the Cynthia and George Mitchell Foundation, and the U.S. Department of Energy's Office of Science through the AmeriFlux Management Project (DE-AC02-05CH11231).

https://doi.org/10.5194/egusphere-2025-2849
Preprint. Discussion started: 4 July 2025

References

Baniya, B., Kim, D., Nkrumah, M., Miao, G., Ono, M., Sarpong, C., & Noormets, A. (2025). *Non-structural carbon dynamics in a shortleaf pine forest during regular and drought years*.

Bond-Lamberty, B., Bronson, D., Bladyka, E., & Gower, S. T. (2011). A comparison of trenched plot techniques for partitioning soil respiration. *Soil Biology and Biochemistry*, *43*(10), 2108-2114. https://doi.org/https://doi.org/10.1016/j.soilbio.2011.06.011

Braga, S. R., Oliveira, M. L. R. d., & Gorgens, E. B. (2023). *forestmangr: Forest Mensuration and Management*. In (Version 0.9.6) https://CRAN.R-project.org/package=forestmangr

Canarini, A., Kaiser, C., Merchant, A., Richter, A., & Wanek, W. (2019). Root Exudation of Primary Metabolites: Mechanisms and Their Roles in Plant Responses to Environmental Stimuli [Review]. *Frontiers in plant science*, *10*. https://doi.org/10.3389/fpls.2019.00157

Davidson, E. A., Belk, E., & Boone, R. D. (1998). Soil water content and temperature as independent or confounded factors controlling soil respiration in a temperate mixed hardwood forest. *Global Change Biology*, *4*(2), 217-227. https://doi.org/10.1046/j.1365-2486.1998.00128.x

Davidson, E. A., Janssens, I. A., & Luo, Y. (2006). On the variability of respiration in terrestrial ecosystems: moving beyond Q_{10}. *Global Change Biology*, *12*(2), 154-164. https://doi.org/10.1111/j.1365-2486.2005.01065.x

Fenn, K. M., Malhi, Y., & Morecroft, M. D. (2010). Soil CO_2 efflux in a temperate deciduous forest: Environmental drivers and component contributions. *Soil Biology and Biochemistry*, *42*(10), 1685-1693. https://doi.org/10.1016/j.soilbio.2010.05.028

Friedlingstein, P., O'Sullivan, M., Jones, M. W., Andrew, R. M., Gregor, L., Hauck, J., Le Quéré, C., Luijkx, I. T., Olsen, A., Peters, G. P., Peters, W., Pongratz, J., Schwingshackl, C., Sitch, S., Canadell, J. G., Ciais, P., Jackson, R. B., Alin, S. R., Alkama, R.,…Zheng, B. (2022). Global Carbon Budget 2022. *Earth Syst. Sci. Data*, *14*(11), 4811-4900. https://doi.org/10.5194/essd-14-4811-2022

Gessler, A., Keitel, C., Kodama, N., Weston, C., Winters, A. J., Keith, H., Grice, K., Leuning, R., & Farquhar, G. D. (2007). $\delta^{13}C$ of organic matter transported from the leaves to the roots in *Eucalyptus delegatensis*: short-term variations and relation to respired CO_2. *Functional Plant Biology*, *34*(8), 692-706. https://doi.org/10.1071/FP07064

Gessler, A., & Zweifel, R. (2024). Beyond source and sink control – toward an integrated approach to understand the carbon balance in plants. *New Phytologist*, *n/a*(n/a). https://doi.org/10.1111/nph.19611

Grinsted, A., Moore, J. C., & Jevrejeva, S. (2004). Application of the cross wavelet transform and wavelet coherence to geophysical time series. *Nonlinear Processes in Geophysics*, *11*(5/6), 561-566. https://doi.org/10.5194/npg-11-561-2004

Hagenbo, A., Hadden, D., Clemmensen, K. E., Grelle, A., Manzoni, S., Molder, M., Ekblad, A., & Fransson, P. (2019). Carbon use efficiency of mycorrhizal fungal mycelium increases during the growing season but decreases with forest age across a *Pinus sylvestris* chronosequence. *Journal of Ecology*, *107*(6), 2808-2822. https://doi.org/10.1111/1365-2745.13209

Han, G., Luo, Y., Li, D., Xia, J., Xing, Q., & Yu, J. (2014). Ecosystem photosynthesis regulates soil respiration on a diurnal scale with a short-term time lag in a coastal wetland. *Soil Biology and Biochemistry*, *68*, 85-94. https://doi.org/10.1016/j.soilbio.2013.09.024

Hashimoto, S., Ito, A., & Nishina, K. (2023). Divergent data-driven estimates of global soil respiration. *Communications Earth & Environment*, *4*(1), 460. https://doi.org/10.1038/s43247-023-01136-2

Heinemeyer, A., Wilkinson, M., Vargas, R., Subke, J. A., Casella, E., Morison, J. I. L., & Ineson, P. (2012). Exploring the "overflow tap" theory: linking forest soil CO_2 fluxes and individual mycorrhizosphere components to photosynthesis. *Biogeosciences*, *9*(1), 79-95. https://doi.org/10.5194/bg-9-79-2012

Herms, D. A., & Mattson, W. J. (1992). The Dilemma of Plants: To Grow or Defend. *The Quarterly Review of Biology*, *67*(3), 283-335. https://doi.org/10.1086/417659

Högberg, P., Högberg, M. N., Göttlicher, S. G., Betson, N. R., Keel, S. G., Metcalfe, D. B., Campbell, C., Schindlbacher, A., Hurry, V., Lundmark, T., Linder, S., & Näsholm, T. (2008). High temporal resolution tracing of photosynthate carbon from the tree canopy to forest soil microorganisms. *New Phytologist*, *177*(1), 220-228. https://doi.org/10.1111/j.1469-8137.2007.02238.x

https://doi.org/10.5194/egusphere-2025-2849
Preprint. Discussion started: 4 July 2025

Jian, J., Vargas, R., Anderson-Teixeira, K. J., Stell, E., Herrmann, V., Horn, M., Kholod, N., Manzon, J., Marchesi, R., Paredes, D., & Bond-Lamberty, B. P. (2021). A Global Database of Soil Respiration Data, Version 5.0. In: ORNL Distributed Active Archive Center.

Jiang, M., Medlyn, B. E., Drake, J. E., Duursma, R. A., Anderson, I. C., Barton, C. V. M., Boer, M. M., Carrillo, Y., Castañeda-Gómez, L., Collins, L., Crous, K. Y., De Kauwe, M. G., dos Santos, B. M., Emmerson, K. M., Facey, S. L., Gherlenda, A. N., Gimeno, T. E., Hasegawa, S., Johnson, S. N.,…Ellsworth, D. S. (2020). The fate of carbon in a mature forest under carbon dioxide enrichment. *Nature*, *580*(7802), 227-231. https://doi.org/10.1038/s41586-020-2128-9

Jilling, A., Keiluweit, M., Gutknecht, J. L. M., & Grandy, A. S. (2021). Priming mechanisms providing plants and microbes access to mineral-associated organic matter. *Soil Biology and Biochemistry*, *158*, 108265. https://doi.org/10.1016/j.soilbio.2021.108265

Klein, T., Bader, M. K. F., Leuzinger, S., Mildner, M., Schleppi, P., Siegwolf, R. T. W., & Körner, C. (2016). Growth and carbon relations of mature *Picea abies* trees under 5 years of free-air CO_2 enrichment. *Journal of Ecology*, *104*(6), 1720-1733. https://doi.org/10.1111/1365-2745.12621

Kodama, N., Barnard, R. L., Salmon, Y., Weston, C., Ferrio, J. P., Holst, J., Werner, R. A., Saurer, M., Rennenberg, H., Buchmann, N., & Gessler, A. (2008). Temporal dynamics of the carbon isotope composition in a *Pinus sylvestris* stand: from newly assimilated organic carbon to respired carbon dioxide. *Oecologia*, *156*(4), 737-750. https://doi.org/10.1007/s00442-008-1030-1

Körner, C. (2015). Paradigm shift in plant growth control. *Current Opinion in Plant Biology*, *25*, 107-114. https://doi.org/10.1016/j.pbi.2015.05.003

Kuzyakov, Y. (2010). Priming effects: Interactions between living and dead organic matter. *Soil Biology and Biochemistry*, *42*(9), 1363-1371. https://doi.org/10.1016/j.soilbio.2010.04.003

Kuzyakov, Y., & Gavrichkova, O. (2010). REVIEW: Time lag between photosynthesis and carbon dioxide efflux from soil: a review of mechanisms and controls. *Global Change Biology*, *16*(12), 3386-3406. https://doi.org/10.1111/j.1365-2486.2010.02179.x

Lawrence, D. M., Fisher, R. A., Koven, C. D., Oleson, K. W., Swenson, S. C., Bonan, G., Collier, N., Ghimire, B., van Kampenhout, L., Kennedy, D., Kluzek, E., Lawrence, P. J., Li, F., Li, H., Lombardozzi, D., Riley, W. J., Sacks, W. J., Shi, M., Vertenstein, M.,…Zeng, X. (2019). The Community Land Model Version 5: Description of New Features, Benchmarking, and Impact of Forcing Uncertainty. *Journal of Advances in Modeling Earth Systems*, *11*(12), 4245-4287. https://doi.org/10.1029/2018MS001583

Li, H.-j., Yan, J.-x., Yue, X.-f., & Wang, M.-b. (2008). Significance of soil temperature and moisture for soil respiration in a Chinese mountain area. *Agricultural and Forest Meteorology*, *148*(3), 490-503. https://doi.org/10.1016/j.agrformet.2007.10.009

Liu, Q., Edwards, N. T., Post, W. M., Gu, L., Ledford, J., & Lenhart, S. (2006). Temperature-independent diel variation in soil respiration observed from a temperate deciduous forest. *Global Change Biology*, *12*(11), 2136-2145. https://doi.org/10.1111/j.1365-2486.2006.01245.x

Lloyd, J., & Taylor, J. A. (1994). On the Temperature Dependence of Soil Respiration. *Functional Ecology*, *8*(3), 315-323. https://doi.org/10.2307/2389824

Martin, J. G., Phillips, C. L., Schmidt, A., Irvine, J., & Law, B. E. (2012). High-frequency analysis of the complex linkage between soil CO_2 fluxes, photosynthesis and environmental variables. *Tree Physiology*, *32*(1), 49-64. https://doi.org/10.1093/treephys/tpr134

McElligott, K. M., Seiler, J. R., & Strahm, B. D. (2016). Partitioning soil respiration across four age classes of loblolly pine (*Pinus taeda* L.) on the Virginia Piedmont. *Forest Ecology and Management*, *378*, 173-180. https://doi.org/10.1016/j.foreco.2016.07.026

Meier, I. C., Finzi, A. C., & Phillips, R. P. (2017). Root exudates increase N availability by stimulating microbial turnover of fast-cycling N pools. *Soil Biology and Biochemistry*, *106*, 119-128. https://doi.org/10.1016/j.soilbio.2016.12.004

Mencuccini, M., & Hölttä, T. (2010). The significance of phloem transport for the speed with which canopy photosynthesis and belowground respiration are linked. *New Phytologist*, *185*(1), 189-203. https://doi.org/10.1111/j.1469-8137.2009.03050.x

https://doi.org/10.5194/egusphere-2025-2849
Preprint. Discussion started: 4 July 2025

Mitra, B., Miao, G., Minick, K., McNulty, S. G., Sun, G., Gavazzi, M., King, J. S., & Noormets, A. (2019). Disentangling the Effects of Temperature, Moisture, and Substrate Availability on Soil CO_2 Efflux. *Journal of Geophysical Research: Biogeosciences*, *124*(7), 2060-2075. https://doi.org/10.1029/2019jg005148

Moyano, F. E., Kutsch, W. L., & Rebmann, C. (2008). Soil respiration fluxes in relation to photosynthetic activity in broad-leaf and needle-leaf forest stands. *Agricultural and Forest Meteorology*, *148*(1), 135-143. https://doi.org/10.1016/j.agrformet.2007.09.006

Myneni, R., Knyazikhin, Y., & Park, T. (2021). *MODIS/Terra+Aqua Leaf Area Index/FPAR 4-Day L4 Global 500m SIN Grid V061* (https://doi.org/10.5067/MODIS/MCD15A3H.061

Noormets, A. (2024). *AmeriFlux BASE US-CRK Davy Crockett National Forest* (Version 5-5) AmeriFlux AMP. https://doi.org/10.17190/AMF/2204055

O'Sullivan, M., Friedlingstein, P., Sitch, S., Anthoni, P., Arneth, A., Arora, V. K., Bastrikov, V., Delire, C., Goll, D. S., Jain, A., Kato, E., Kennedy, D., Knauer, J., Lienert, S., Lombardozzi, D., McGuire, P. C., Melton, J. R., Nabel, J. E. M. S., Pongratz, J.,…Zaehle, S. (2022). Process-oriented analysis of dominant sources of uncertainty in the land carbon sink. *Nature Communications*, *13*(1), 4781. https://doi.org/10.1038/s41467-022-32416-8

Ono, M. (2025). *Software from: The Use of Newly Assimilated Photosynthates by Soil Autotrophic and Heterotrophic Respiration on a Diurnal Scale*. In https://github.com/moekaono/CRK_cont_SR

Ono, M., Noormets, A., & Mitchell, S. (2025). The effect of the frequency of prescribed burning on annual soil carbon balance in a loblolly-shortleaf pine forest in East Texas. *Frontiers in Forests and Global Change*, *8*. https://doi.org/10.3389/ffgc.2025.1602557

Phillips, R. P., Erlitz, Y., Bier, R., & Bernhardt, E. S. (2008). New approach for capturing soluble root exudates in forest soils. *Functional Ecology*, *22*(6), 990-999. https://doi.org/10.1111/j.1365-2435.2008.01495.x

Posit team. (2024). *RStudio: Integrated Development Environment for R*. In (Version 2023.12.1.402) Posit Software, PBC. http://www.posit.co/

Prescott, C. E. (2022). Sinks for plant surplus carbon explain several ecological phenomena. *Plant and Soil*. https://doi.org/10.1007/s11104-022-05390-9

Prescott, C. E., Grayston, S. J., Helmisaari, H.-S., Kaštovská, E., Körner, C., Lambers, H., Meier, I. C., Millard, P., & Ostonen, I. (2020). Surplus Carbon Drives Allocation and Plant–Soil Interactions. *Trends in Ecology & Evolution*, *35*(12), 1110-1118. https://doi.org/10.1016/j.tree.2020.08.007

R Core Team. (2024). *R: A Language and Environment for Statistical Computing*. In R Foundation for Statistical Computing. https://www.R-project.org/

Reichstein, M., Falge, E., Baldocchi, D., Papale, D., Aubinet, M., Berbigier, P., Bernhofer, C., Buchmann, N., Gilmanov, T., Granier, A., Grünwald, T., Havránková, K., Ilvesniemi, H., Janous, D., Knohl, A., Laurila, T., Lohila, A., Loustau, D., Matteucci, G.,…Valentini, R. (2005). On the separation of net ecosystem exchange into assimilation and ecosystem respiration: review and improved algorithm. *Global Change Biology*, *11*(9), 1424-1439. https://doi.org/10.1111/j.1365-2486.2005.001002.x

Roesch, A., & Schmidbauer, H. (2018). *WaveletComp: Computational Wavelet Analysis*. In (Version 1.1) https://CRAN.R-project.org/package=WaveletComp

Savage, K., Davidson, E. A., & Tang, J. (2013). Diel patterns of autotrophic and heterotrophic respiration among phenological stages. *Global Change Biology*, *19*(4), 1151-1159. https://doi.org/10.1111/gcb.12108

Sevanto, S., & Dickman, L. T. (2015). Where does the carbon go?—Plant carbon allocation under climate change. *Tree Physiology*, *35*(6), 581-584. https://doi.org/10.1093/treephys/tpv059

Tang, J., Baldocchi, D. D., & Xu, L. (2005). Tree photosynthesis modulates soil respiration on a diurnal time scale. *Global Change Biology*, *11*(8), 1298-1304. https://doi.org/10.1111/j.1365-2486.2005.00978.x

Thompson, M. V., & Holbrook, N. M. (2004). Scaling phloem transport: information transmission. *Plant, Cell & Environment*, *27*(4), 509-519. https://doi.org/10.1111/j.1365-3040.2003.01148.x

van't Hoff, J. H. (1898). *Lectures on theoretical and physical chemistry Part I. chemical dynamics* (R. A. Lehfeldt, Trans.). E. Arnold.

Vargas, R., Baldocchi, D. D., Bahn, M., Hanson, P. J., Hosman, K. P., Kulmala, L., Pumpanen, J., & Yang, B. (2011). On the multi-temporal correlation between photosynthesis and soil CO_2 efflux: reconciling lags and observations. *New Phytol*, *191*(4), 1006-1017. https://doi.org/10.1111/j.1469-8137.2011.03771.x

https://doi.org/10.5194/egusphere-2025-2849
Preprint. Discussion started: 4 July 2025

Wingate, L., Ogée, J., Burlett, R., Bosc, A., Devaux, M., Grace, J., Loustau, D., & Gessler, A. (2010). Photosynthetic carbon isotope discrimination and its relationship to the carbon isotope signals of stem, soil and ecosystem respiration. *New Phytologist*, *188*(2), 576-589. https://doi.org/10.1111/j.1469-8137.2010.03384.x

Wutzler, T., Reichstein, M., Moffat, A. M., & Migliavacca, M. (2022). *REddyProc: Post Processing of (Half-)Hourly Eddy-Covariance Measurements. R package version 1.3.2.* In https://CRAN.R-project.org/package=REddyProc

Yin, H., Wheeler, E., & Phillips, R. P. (2014). Root-induced changes in nutrient cycling in forests depend on exudation rates. *Soil Biology and Biochemistry*, *78*, 213-221. https://doi.org/10.1016/j.soilbio.2014.07.022

Zweifel, R., Sterck, F., Braun, S., Buchmann, N., Eugster, W., Gessler, A., Häni, M., Peters, R. L., Walthert, L., Wilhelm, M., Ziemińska, K., & Etzold, S. (2021). Why trees grow at night. *New Phytologist*, *231*(6), 2174-2185. https://doi.org/10.1111/nph.17552